Xie et al. Herit Sci (2021) 9:122
https://doi.org/10.1186/s40494-021-00594-1

Heritage Science

RESEARCH ARTICLE Open Access

Nano-materials enhanced protectants for natural stone surfaces

Zaixin Xie[1], Zhuoqi Duan[1], Zhanqiang Zhao[1], Ruheng Li[1], Bao Zhou[1], Dequan Yang[2] and Yongmao Hu[1*]

Abstract

Most heritage buildings and monuments are constructed out of natural stones which suffer irrevocable degradation when undergoing wet weathering, bowing, and dissolution in outdoor conditions. Self-cleaning treatments are effective for stone protecting. Herein, nano-materials which provide enhanced protectants for Marble, Qingshi and Hedishi were prepared. Inherent microscale interstices and holes exist on polished natural stone surfaces. When treated by a commercial protectant, 101S, the surfaces were hydrophobic but not self-cleaning. Colloidal protectants were prepared by dispersion of Al_2O_3 and SiO_2 nano-powder in 101S, respectively. Self-cleaning stone surfaces were achieved after treated by the protectants, meanwhile, the interstices and holes were reserved as much as possible. The principle of the as- prepared protectants is penetrating and crosslinking on the stone surfaces as well as the inner surfaces of the interstices and holes. The reserving of the micro interstices and holes is important since the breathability of the stones is remained. The self-cleaning surfaces showed good thermal stability below 250 °C. Meanwhile, changes of color and gloss of the treated stone surfaces are in the acceptable range.

Keywords: Natural stone, Nanomaterial enhanced protectant, Hierarchical structure, Self-cleaning

Introduction

Heritage is one of the most important assets with significant cultural and economic value. Most heritage buildings and monuments are constructed out of natural stones due to their earth-abundance, robustness and harmlessness. In outdoor conditions, natural stones suffer irrevocable degradation when undergoing wet weathering, bowing and dissolution [1, 2]. Generally, rain has a pH value varying from 5.6 where acidity results from ambient CO_2 in normal conditions, to 4.5 in areas polluted by SO_2 and NO_x [3]. The dissolution rate of salts such as calcite and magnesite increases with decreasing of the pH level of the invaded water. Water containing acidic species invades through the micro interstices and holes are harmful due to the crystallization-dissolution cycles of the soluble salts in the stones which induce tensions inside the porous matrix, thus accelerating its decay [3, 4]. Hence, studies on conservation of cultural heritage, especially of natural stones are significant for its future continuation.

Two strategies are employed in the field of stone conservation, i.e., consolidation and surface protection [5–11]. Consolidating treatments aim at improving the cohesion of degraded stones. Alkoxysilanes, tetraethoxysilane (TEOS) and methyltrimethoxysilane (MTMOS) based organic protectants are dominant in the consolidating practices, mainly due to their ability to penetrate easily into porous materials and the light impact on the permeability and drying properties of the stones. The main issues with such products include cracking during the drying due to gel shrinkage, temporary hydrophobic behavior, influence of the ambient humidity on the gel polymerization and poor chemical affinity between protectants and the stone substrates [12, 13]. Inorganic consolidating products, such as calcium hydroxide, barium hydroxide and ammonium oxalate have good durability and compatibility with stone components [14–16]. By using these products, lower penetrability and subsequent

*Correspondence: yongmaohu@163.com
[1] College of Engineering, Dali University, Dali 671003, China
Full list of author information is available at the end of the article

poor strengthening effects should be considered. In recent years, colloidal dispersions containing silica and calcium, magnesium, strontium hydroxides nanoparticles were used for stone consolidation [17–21]. Although great improvements had been achieved, a high level of risk may be posed, e.g., introduction of the products into the porous network may strongly change the stone characteristics and properties, thus causing unwanted effects or further damage. Other issues may be encompassed in consolidation treatments. Consolidates made of water colloidal suspension of nanosilica were applied on a porous limestone. The stone cohesion was improved by the penetration and consolidation of the consolidates, however, a decrease of durability under a salt crystallization test of the treated stone was found, suggesting that the distribution of the nanoparticle fillers into the stone substrate should be improved [12]. Besides, the efficacy of consolidation with colloidal dispersions strongly depends on humidity and climatic fluctuation [13].

For the surface protection strategy, treatments applied on the cortical portion of the stones and water-repellency had been considered [22–24]. Enclosed coatings of acrylic, acryl-siliconic and epoxy resin as well as paraffin were generally adopted [25–31]. Although these coatings can effectively isolate the pollution sources, the breathability, or the water vapor permeability, of the stones might be greatly weakened especially when a high amount of these coatings are applied. As a consequence, with the variation of the ambient temperature, the sealed moisture inside the stones experience cycles of salts crystallization-dissolution which will also accelerate the decay of the stones. In heavily salt-laden cases, simple application of seal coatings can even increase the deterioration rate of the treated stones, leading eventually to flake, scale, and cracking [32]. Moreover, the durability of this kind of coatings is limited due to the relatively weak adhesion with the stone substrates. Hence, protectants combine water repellence, robust adhesion and breathability maintenance is in need.

Self-cleaning surfaces are effective for natural stone protection due to the excellent water repellence and breathability maintaining possibility [22, 33]. A combination of micro-nano roughness and low-surface-energy chemicals derivatization is necessary to self-cleaning surfaces [33, 34]. Inherent micro roughness existed on polished natural stone surfaces, and addition of nano particles in protectants is effective for nanoscale roughness construction. Silica nanoparticles were added in polyalkylsiloxane and water static contact angle (SCA) of 160° on treated Marble surface was obtained [18]. Another protectant was prepared by adding nano $CaCO_3$ nanoparticles in copolymer of epoxy and acrylate [35–37]. Performances of robustness, abrasion, contamination resistance, weathering resistance, and durability of natural stones protected by nanomaterials enhanced protectants (NMEPs) have been greatly improved. Meanwhile, the antibacterial and antifungus properties were enhanced as well.

In present work, an approach to NMEPs was developed. Al_2O_3 and SiO_2 nano-particles were dispersed in a commercial water-resistant coating, 101S, to prepare colloidal protectants. Protectant layers were formed by dip-coating on natural Marble, Qingshi and Hedishi stone surfaces as well as the inner surfaces of interstices and holes beneath the surfaces of several micrometers through pernetrating and crosslinking. Water resistance of the stone surfaces was greatly improved without heavily sacrificing the breathability of the stones. Self-cleaning surfaces were achieved with water SCA of bigger than 150° and hysteresis angles (HAs) less than 20°. The self-cleaning surfaces showed good thermal stability below 250 °C. Meanwhile, changes of color and gloss of the treated stone surfaces are in the acceptable range.

Experimental

Materials and sample preparation

Bulk natural stones of Marble, Qingshi and Hedishi were obtained from the local area of Dali prefecture, Yunnan province, China. Commercial water-resistant coating, 101S, was obtained from Solmont Technology (Shenzhen) Co., Ltd. 101 s is a clear and transparent liquid coating with a surface tension of 14 mN/m (at 20 °C), mainly composed by perfluoroalkylpolyether (PFPE) in which $–CF_2$ and $–CF_3$ are the water-repellent groups. The coating can easily penetrate into interstices and holes inside natural stones to form a water repellant layer via crosslink at room temperature in air within 48 h. Al_2O_3 (99.9%, 30 nm) and SiO_2 (99.5%, 15 nm) nano-powders were bought from Shanghai Macklin Biochemical Technology Co., Ltd and Shanghai Aladdin Bio-Chem Technology Co., Ltd, respectively.

The stones were cut into 50 mm × 15 mm × 5 mm coupons. Double faces of each coupon were primarily polished by 400# grinding wheels and pasted on glass slides by UV curing adhesive. Surfaces of natural stone specimens were prepared by sequentially polishing the coupon surfaces by 1200# grinding wheels and polishing cloth followed by a 15 min ultrasonic washing in ethanol and DI water (18.2 MΩ, MilliQ) respectively to eliminate organic native oxide and contaminations. The specimens were dried for 24 h under 40 °C in a drying box followed by a 3 min UV-ozone cleaning prior to treatment.

The nano-powders were heated at 100 °C on a heating plate for 1 h to eliminate moistures prior to use. Colloidal dispersion protectants were prepared as follows. Concentrations of 0.1 mg/mL, 0.5 mg/mL, 1.0 mg/mL, 1.5 mg/

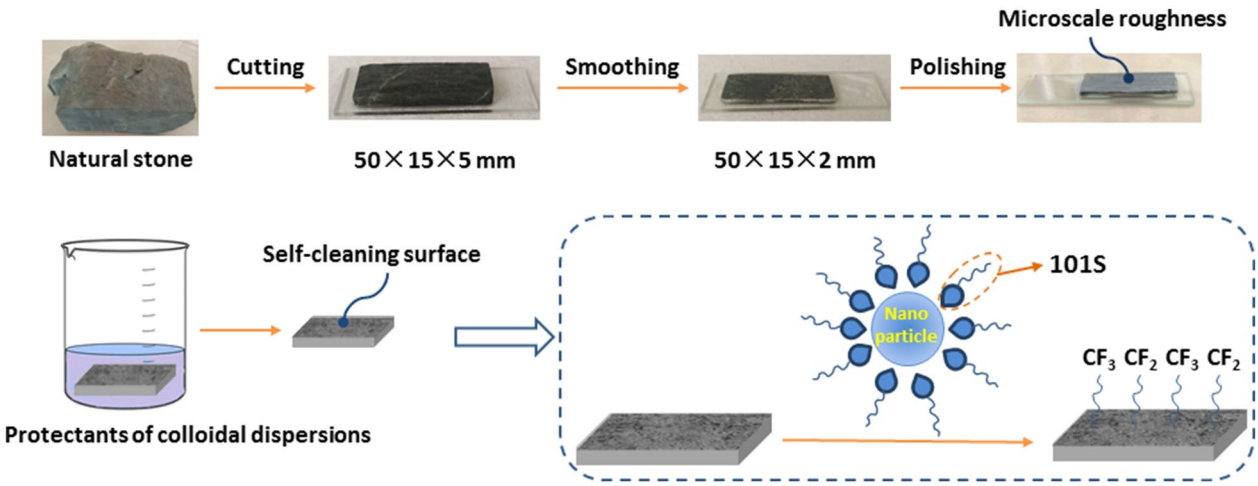

Fig. 1 Schematic diagram of the preparation of the natural stone surfaces (upper), and treatment of stone surfaces with colloidal dispersion protectant (lower)

mL and 2.0 mg/mL of Al_2O_3 and SiO_2 nanoparticles were dispersed into the 101S liquid respectively by a five ultrasonic dispersion periods followed by a magnetic stirring for 2.5 h. In each period, alternated ultrasonic of 28 kHz and 40 kHz for 5 min were adopted. The cleaned natural stone specimens were immersed into the protectants for 14 h and dried at 40 °C for 24 h. The preparation diagram of the samples is shown in Fig. 1.

Surface characterization

X-ray diffraction (XRD) was employed to analyze the composition of the natural stones. Samples were performed on stainless steel holders in an EMPYREAN, PANalytical, NL with λ = 1.5406 Å of Cu K_α radiation. XRD patterns were recorded by scanning from 5° to 90° with a step of 0.02° and a rate of 0.2°/sec in a continuous mode. The working conditions are 40 kV and 40 mA. Scanning electron microscopy (SEM) images were obtained with a SU8020 on gold-sputtered surfaces under 3.0 kV accelerating voltage, 10^{-5} Torr vacuum and 3.2 mm working distance. Water contact angles (CAs) were measured with a SDC-200 contact angle measurement (CAM) system. All CAMs were carried out with DI water at ambient temperature of 23–25 °C and relative humidity of 60–75%. The volume and diameter of the DI water droplets used are about 3 μL and 0.9 mm, respectively. On each surface, at least five spots were tested and the averaged value was adopted [38, 39]. Thermal stability, breathability and color and gloss changes of the treated surfaces were evaluated and detailed in the following section.

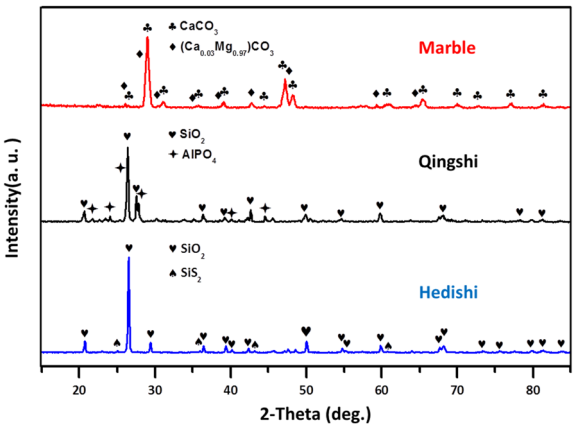

Fig. 2 XRD patterns of natural Marble, Qingshi and Hedishi stones

Results and discussion

Stone composition

XRD patterns of the three natural stones are shown in Fig. 2 and corresponding main ingredients of the stones are summarized in Table 1. The dominant ingredient of Marble is $CaCO_3$, while that of Qingshi and Hedishi is SiO_2. Graphite and ferric oxides exist in the stones of Qingshi and Hedishi. However, the amount of these species is too small to be detected by XRD.

Water repellence of 101S

In order to evaluate water repellence of 101S, and minimize the affection of surface roughness, water CAs of blank and 101S coated glass surfaces were measured and summarized in Table 2. Water SCA of 62.6 ± 0.3°

Table 1 Main ingredients of natural Marble, Qingshi and Hedishi stones, and the corresponding peak locations in XRD patterns

Stone	component	Location (2θ)
Marble	$CaCO_3$	23.05, 29.40, 35.97, 39.41, 43.16, 47.11, 48.503, 60.67, 65.61, 70.24, 73.73, 77.18, 81.55, 83.77
	$(Ca_{0.03}Mg_{0.97})CO_3$	23.12, 29.50, 36.06, 39.52, 43.27, 47.25, 47.70, 48.13, 49.06
	Cu_2FeGeS_4	29.15, 48.30, 48.65, 57.42
Qingshi	SiO_2	20.83, 26.59, 36.50, 39.37, 40.23, 42.39, 50.03, 55.17, 59.86, 68.20, 68.32, 73.47, 75.66, 79.88, 80.04, 81.17, 81.49
	$AlPO_4$	20.76, 26.43, 36.37, 39.06, 40.71, 59.61, 67.23, 67.36, 67.80, 72.48, 80.92
	C	26.55, 44.57, 54.54
Hedishi	SiO_2	20.86, 26.64, 36.54, 39.46, 40.29, 42.45, 45.788, 50.13, 54.87, 59.95, 65.78, 67.74, 68.14, 68.32, 73.47, 75.66, 77.67, 79.88, 80.04, 81.17, 81.49, 83.84, 84.96
	SiS_2	20.79, 26.51, 36.50, 39.49, 42.40, 50.08, 54.935, 60.02, 68.32

Table 2 Water SCAs, advancing contact angles (ACAs), receding contact angles (RCAs) on glass and natural stone surfaces and corresponding HAs before and after 101S treatment

Surface	Blank	With 101S modification			
	SCA (°)	SCA (°)	ACA (°)	RCA (°)	HA (°)
Glass	62.6 ± 0.3	118.0 ± 0.5	128.0 ± 0.6	103.1 ± 0.5	24.9
Marble	53.0 ± 0.7	139.3 ± 0.6	148.0 ± 0.4	114.0 ± 0.3	34.1
Qingshi	38.3 ± 0.6	137.0 ± 0.7	141.0 ± 0.6	93.6 ± 0.7	47.3
Hedishi	47.0 ± 0.7	133.6 ± 0.8	137.9 ± 0.5	111.0 ± 0.8	26.9

was obtained on the hydrophilic blank glass surface. It increased to 118 ± 0.5° after coated with 101S, while the hysteresis angle (HA) is 24.9°. The water repellence component of 101S is perfluoroalkylpolyether (PFPE) in which $-CF_2$ and $-CF_3$ are the functional groups. The result agrees well with the maximum contact angle of about 120° what can be obtained on a flat surface derived by groups of $-CF_2$ and $-CF_3$ [40].

All polished stone surfaces are hydrophilic with water SCAs of 53 ± 0.7°, 38 ± 0.6° and 47 ± 0.7°, respectively. After coated by 101S, the SCAs increase to 139 ± 0.6°, 137 ± 0.7° and 134 ± 0.8°, meanwhile the HAs are 34°, 47° and 27°, respectively.

Numerous micro holes and interstices existed on and beneath the natural stone surfaces. Liquid 101S can easily penetrate into the interstices and holes due to its low surface tension of 14 mN/m (20 °C), and then crosslinked on the stone surfaces as well as the inner surfaces of the interstices and holes. The inherent microscale roughness enhanced the water repellence. However, a difference existed from self-cleaning surfaces which require water sliding angle less than 5° (or the HA less than 20°). Self-cleaning surfaces cannot be achieved by 101S treatments and can only be achieved by a combination of low-surface-energy chemicals and surface micro-nano structures.

Surface wettability

Wettability of stone surfaces treated with Al_2O_3 nano-powder added 101S

The concentrations of the Al_2O_3 nano-powder added in 101S are 0.1 mg/mL, 0.5 mg/mL, 1.0 mg/mL, 1.5 mg/mL and 2.0 mg/mL. Figure 3a–c present variations of water CAs on the treated stone surfaces with the concentration of the Al_2O_3 nano-powder. For Marble surfaces (Fig. 2a), when 0.1 mg/mL was dispersed into 101S, water SCA is 166.5°, significantly increased compared with that of 139.3° on the surface treated by pure 101S. Meanwhile, the HA decreases from 34.1° to 11.2°. The SCA continuously increases to the maximum value of 171.2° with the concentration to 1.5 mg/mL. When the concentration of Al_2O_3 nano-powder reaches to 2.0 mg/mL, the SCA decreases to 166.8°. For the HA, the minimum value obtained when the concentration of Al_2O_3 nano-powder is 0.5 mg/mL, it increases to 14.6° with the concentration of Al_2O_3 nano-powder to 1.5 mg/mL, and then decreases to 12.1°. On the treated Qingshi surfaces, the SCA reaches to 161.7° when 0.1 mg/mL Al_2O_3 nano-powder was added to 101S. The SCA first decreases and then increases with the concentration of Al_2O_3 nano-powder thereafter. The maximum SCA of 169.2° was obtained when the concentration of Al_2O_3 nano-powder is 1.5 mg/mL. The HA various in the range of 11.3°–14.6° with the concentration of Al_2O_3 nano-powder. The treated Hedishi surfaces present excellent water repellence with SCA of 170.3° when 0.5 mg/mL Al_2O_3 nano-powder was added in 101S, meanwhile, the HA is 16.8°, slightly bigger than those on Marble and Qingshi surfaces. In the range of 0.5–2.0 mg/mL, although the SCA slightly decreases with the concentration of Al_2O_3 nano-powder, self-cleaning surfaces were achieved.

The optimal SCAs and corresponding concentration of Al_2O_3 nano-powder are summarized in Fig. 3d. The optimal SCA on treated Qingshi surface is relatively smaller and the corresponding concentration of Al_2O_3

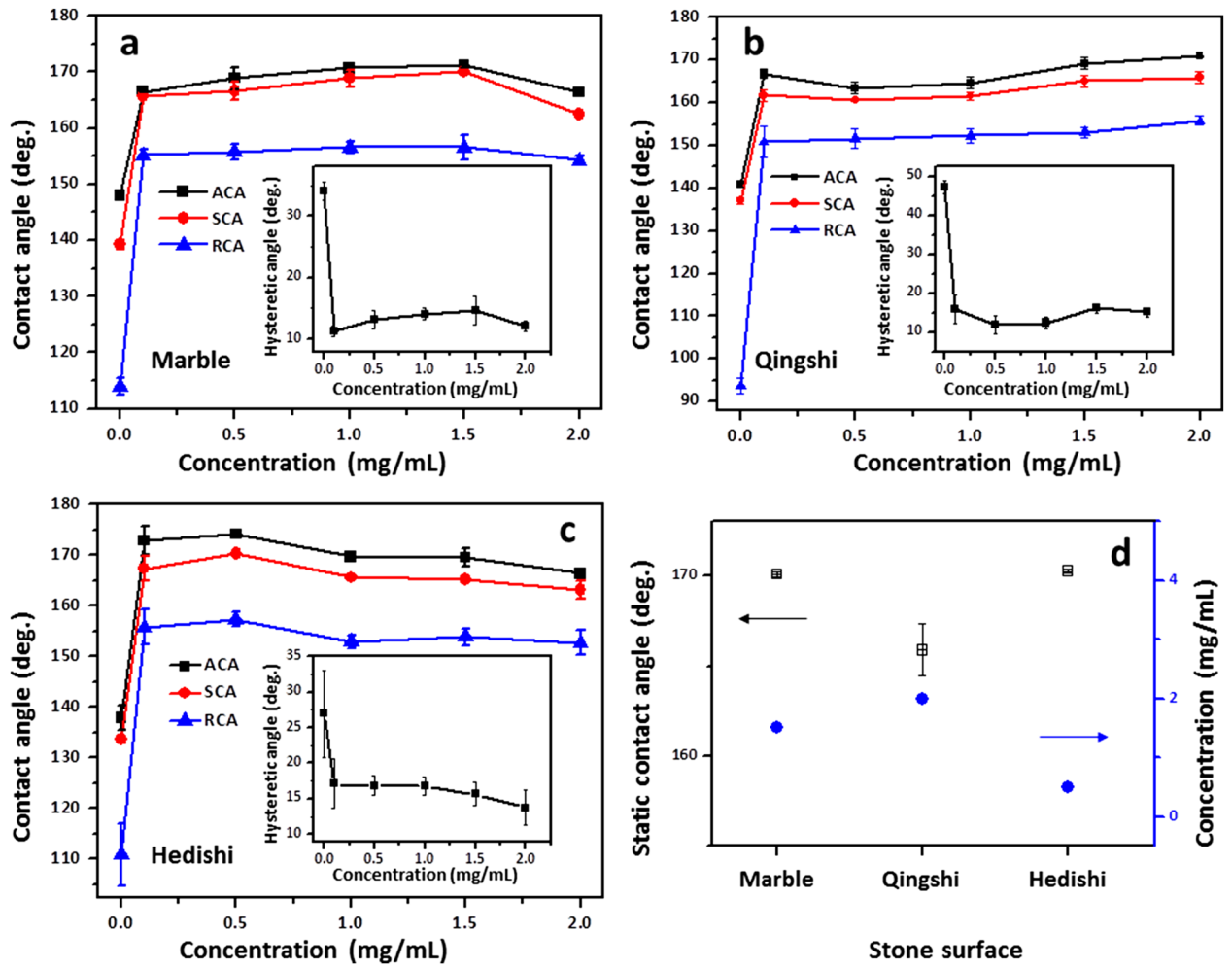

Fig. 3 Variations of water CAs on **a** Marble, **b** Qingshi and **c** Hedishi surfaces treated by the as-prepared protectants with the concentration of Al_2O_3 nano-powder, and d the optimal water SCAs on stone surfaces

nano-powder is bigger than those of treated Marble and Hedishi surfaces. The result is related to the difference of the surface pattern between Qingshi and Marble (and Hedishi) which will be depicted later.

Wettability of stone surfaces treated with SiO_2 nano-powder added 101S

Nano SiO_2 powder was used as another additive to 101S for protectants. Variations of water CAs as a function of the concentration of SiO_2 nano-powder are shown in Fig. 4a–c. Water repellence of the treated Marble surface was significantly improved when 0.1 mg/mL SiO_2 nano-powder was added into 101S, i.e., the SCA increased to 166.7° compared with that of 139.3° in the SiO_2-free case, meanwhile the HA decreased from 34.1° to 11.2°, presenting self-cleaning. This property was maintained in the SiO_2 nano-powder concentration ranging from 0.5 to 2.0 mg/mL with a slightly increase of the HA (Fig. 3a). For the Qingshi surfaces, the variations of the SCA and ACA are similar to those on Marble surfaces. However, the RCA is relatively small in the SiO_2 nano-powder concentration ranging from 0.1 to 0.5 mg/mL. Self-cleaning surfaces were achieved when the concentration reaches to 1.0 mg/mL. The variation of the water CA on treated Hedishi surfaces is similar to that on Marble surfaces. In the whole concentration range of SiO_2 nano-powder surveyed in this work, self-cleaning property is well maintained.

The optimal SCAs and corresponding concentration of SiO_2 nano-powder are summarized in Fig. 4d. Similar to the surfaces treated by Al_2O_3 nano-powder added 101S protectants, the optimal SCA on treated Qingshi surface is relatively smaller and the corresponding concentration of SiO_2 nano-powder is bigger than those on the treated Marble and Hedishi surfaces. We suggest the result is induced by the different patterns of

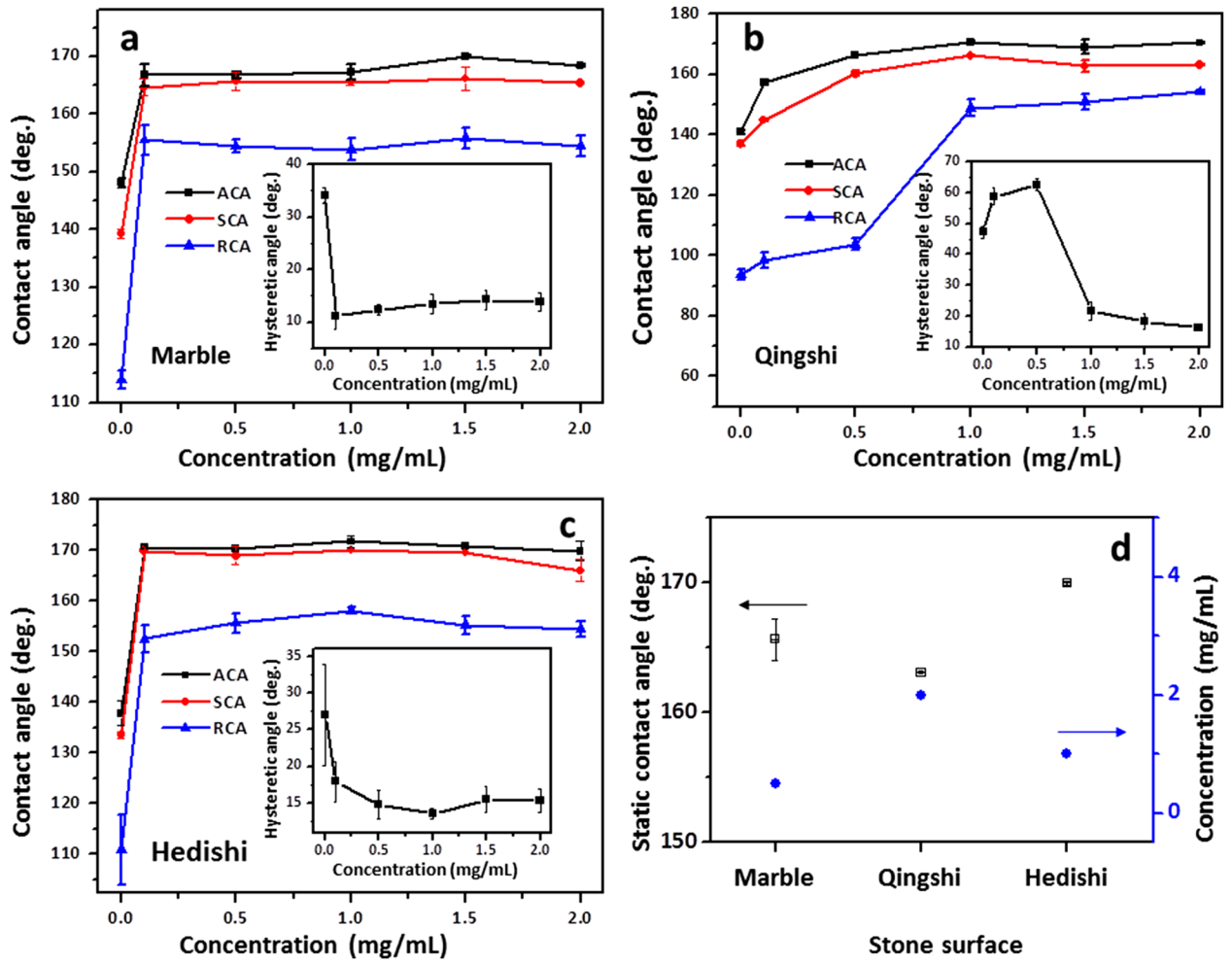

Fig. 4 Variations of water CAs on **a** Marble, **b** Qingshi and **c** Hedishi surfaces treated by the as-prepared protectants with the concentration of SiO_2 nano-powder, and d the optimal water SCAs on the stone surfaces

the Qingshi surfaces from those of Marble and Hedishi surfaces.

It is demonstrated that water repellence of the treated stone surfaces was significantly improved by dispersion of Al_2O_3 and SiO_2 nano-powder in 101S. Self-cleaning surfaces were achieved for all stone specimens except for Qingshi surfaces in the cases of the concentration of SiO_2 nano-powder below 1.0 mg/mL. Numerous micro holes and interstices existed on and beneath the natural stone surfaces. The as-prepared liquid protectants penetrated into the holes and interstices and crosslinked to form a water-resistant layer on the inner surfaces as well as on the outside surface. The addition of Al_2O_3 and SiO_2 nano-powder provides nanoscale roughness on the surfaces. Hence, self-cleaning surfaces were achieved by functions of the 101S and the nanoscale roughness together with the inherent microscale roughness on the stone surfaces.

Mechanism of the water repellence

Based on the Young's equation, Wenzel and Cassie developed two models to explain the influence of surface roughness on the apparent contact angle of liquid droplets. The Wenzel model suggests that surface roughness will increase the actual contact area of the liquid and amplify the wettability of solid surfaces, and the apparent contact angle can be modified as [41, 42]:

$$\cos\theta = r\cos\theta_0 \tag{1}$$

where θ is the apparent contact angle of droplets on the rough surface; r is the surface roughness factor ($r > 1$) which is a measure of how surface roughness affects a homogeneous surface and defined as the ratio of actual contact area with the liquid of the solid surface to the geometric area in contact with the droplet; θ_0 is the equilibrium contact angle of the droplets on an ideal smooth

surface of the same material, given by Young's equation as $\cos\theta_0 = (\gamma_{sv} - \gamma_{sl})/\gamma_{lv}$, where γ refers to the interfacial tension and the subscripts s, l, v refer to the solid, liquid, and vapor phases, respectively. While the Cassie model postulates that a hydrophobic rough surface will trap air bubbles in micro-pockets at the solid–liquid interface, leading to a composite interface, and giving the apparent contact angle as [43, 44]:

$$\cos\theta = f(\cos\theta_0 + 1) - 1 \quad (2)$$

where f is the ratio of the solid area in contact with the liquid to the geometric area in contact with the droplet ($f < 1$).

According to Wenzel model, in order to achieve self-cleaning surfaces, θ_0 must be bigger than 90°, i.e. the solid surface must be hydrophobic. In contrast, the Cassie relation allows for the possibility of $\theta > 90°$ even with $\theta_0 < 90°$ which is generally existed when water droplets contact with hydrophilic solid surfaces. In addition, according to Wenzel model, water will penetrate into the micro-pockets at the solid–liquid interface when contact with solid surfaces. As a consequence, water droplets can hardly sliding or the sliding angle is usually large on the surfaces. Hence, Wenzel model can hardly fulfill the sliding requirement of self-cleaning surfaces, i.e. the sliding angle is less than 5° (or the HA is less than 20°). On the other hand, to achieve Cassie state, low surface tension material is in need. Hence, for self-cleaning surfaces, hierarchical micro/nanometer scale roughness and low surface tension material are necessary.

Figure 5 shows SEM images of Marble surfaces and profiles before and after treated by the protectants. Non-uniform micro interstices and holes exist on the polished blank Marble surface. The width of the interstices as well as the diameter of the holes is in the range of several hundred nanometers, and the length of interstices is mainly several micrometers (Fig. 5a). The depth of these interstices and holes is ranging from nanometers to micrometers (Fig. 5e). The micro interstices and holes almost maintain unchanged after treated with 101S (Fig. 4b and f). During the treatment, the liquid protectants stayed on the Marble surface and penetrated into the interstices and holes, and formed a protective layer after crosslinking of the 101S. The morphology of the Marble surfaces didn't change when covered by the protective layer. That is why the SCA increased from 53° to 139.3° instead of 118°on the 101S covered smooth glass surface. In other word, the microscale roughness on the Marble surface enhanced the water repellence. However, the corresponding HA of 34.1° is relatively big, much below the standard of self-cleaning surfaces. Hence, only microscale roughness on the Marble surface is fall short of the structural request of the self-cleaning surfaces.

When 1.5 mg/mL Al_2O_3 nano-powder was dispersed into 101S, nanoscale embossments formed on the microscale pattern of the Marble surfaces (Fig. 5c and g). Self-cleaning surfaces were obtained by combining the micro-nano roughness and the low surface energy of 101S. The interstices and holes were maintained except a little size decrease after treatment. It is important because stones will breathe through the interstices and holes in ambient environment, i.e., moistures outer and inner the stones can exchange through these interstices and holes and the possible breakdown of the stones induced by ambient temperature will be decreased.

The present of 0.5 mg/mL SiO_2 nano-powder addition is similar to that of Al_2O_3 nano-powder except a little difference of the morphology, i.e., although the size of the

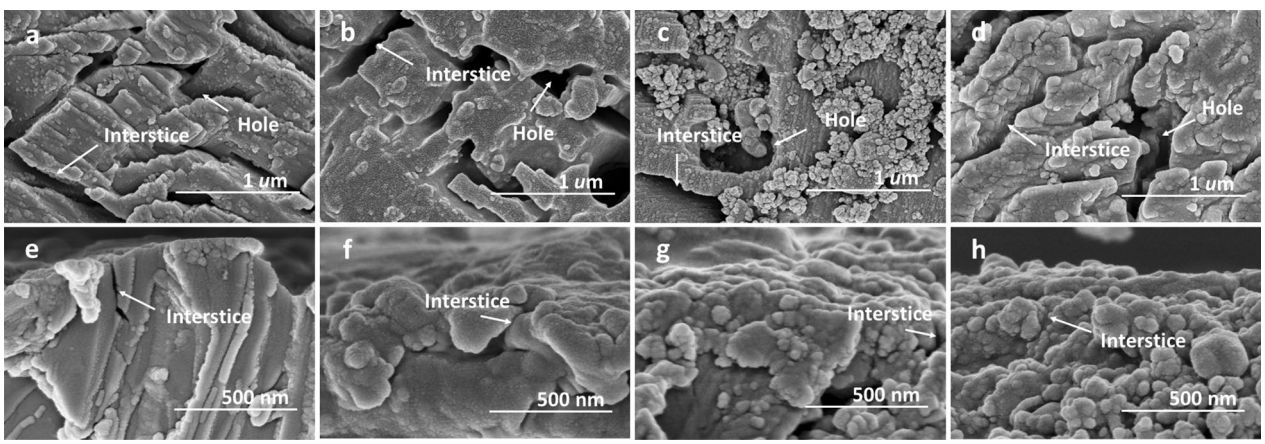

Fig. 5 SEM images of blank (**a** and **e**), and treated by 101S (**b** and **f**), 101S containing 1.5 mg/mL Al_2O_3 nano-powder (**c** and **g**), and 0.5 mg/mL SiO_2 nano-powder (**d** and **h**) Marble surfaces and profiles, respectively

embossments is bigger than that induced by Al_2O_3 nano-powder, the interstices and holes were also maintained (Fig. 5d and h).

SEM images of Qingshi and Hedishi surfaces are shown in Figs. 6 and 7. The morphology of Hedishi surfaces is similar to that of Marbles while the morphology of the Qingshi surfaces presents step-like or fish scale like morphology in which interstices and holes are not distinct. The unique morphology is the reason of the difference request of the nano-powder concentration to self-cleaning from that of Marble and Qingshi.

Based on the models of Wenzel and Cassie [41–44] and the morphology of the stone surfaces above-mentioned, a conclusion that Cassie state of water droplets stay on the self-cleaning surfaces can be drawn. The fraction, f, of the solid in contact with the liquid droplet is calculated according to Eq. (2) and summarized in Fig. 8. The average fraction is about 5%, which is a receivable value of droplets in Cassie state when contact with a solid surface [38–40, 45]. The micro/nanoscale hierarchical structures can trap a large amount of air, which can prevent the penetration of water into the grooves and bestow self-cleaning surfaces.

Water vapor permeability

Porosity and especially the pore space geometry play a great role in the migration of fluids and vapor inside the stones. Small reduction of the pore space in the treated specimens did not have significant influence on the permeability of water vapor [12]. In present work, water vapor permeability was measured by the cup test method. For one kind of stone, two 3 mm thick slices were cut and polished with the same process mentioned above. One slice was treated with the as-prepared protectants, another one was maintained blank as a control specimen. The slices were adhered on cups (with 4 mL

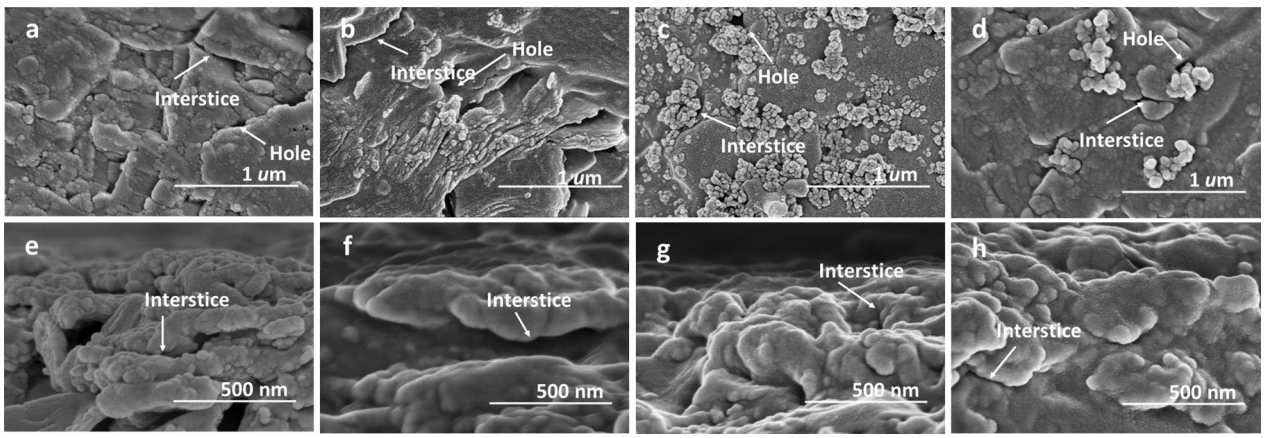

Fig. 6 SEM images of blank (**a** and **e**), and modified by 101S (**b** and **f**), 101S containing 2.0 mg/mL Al_2O_3 nano-powder (**c** and **g**), and 2.0 mg/mL SiO_2 nano-powder (**d** and **h**) Qingshi surfaces and profiles, respectively

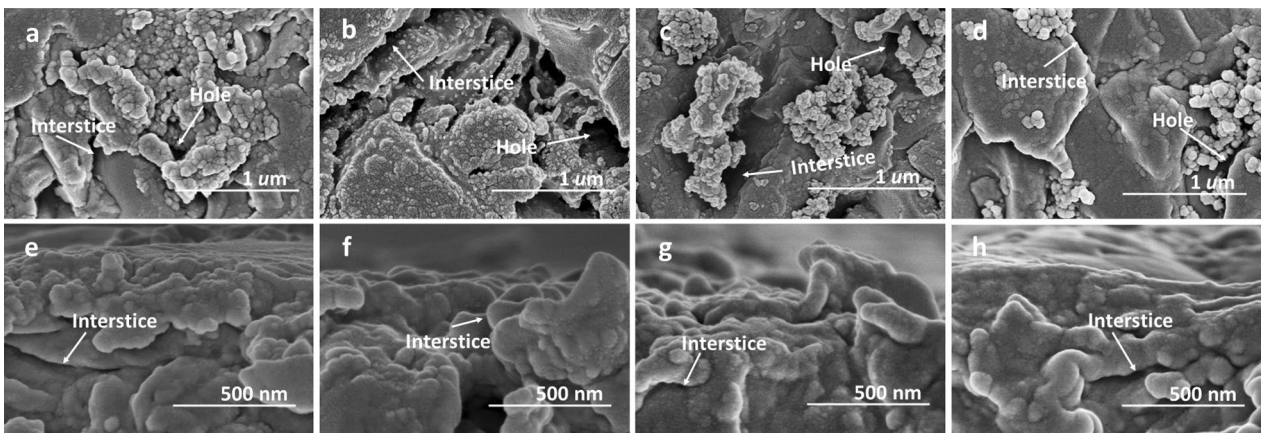

Fig. 7 SEM images of blank (**a** and **e**), and modified by 101S (**b** and **f**), 101S containing 0.5 mg/mL Al_2O_3 nano-powder (**c** and **g**, and 1.0 mg/mL SiO_2 nano-powder (**d** and **h**) Hedishi surfaces and profiles, respectively

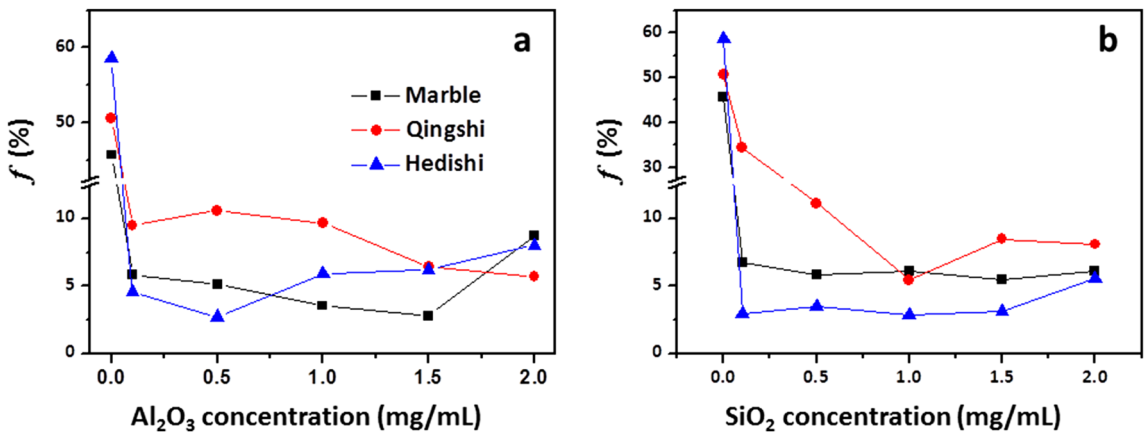

Fig. 8 Fractions of the treated stone surfaces in contact with water droplets calculated based on the Cassie model

DI water inside) by glass cement, acting as the lids. The caliber of the cup is 7 mm. After 48 h solidification of the glass cement, the cups were put into a drying box at 30 °C. Mass of the cups was measured by an electronic balance in every period (24 h each). The experimental diagram is shown in Fig. 9a. Relative mass of the cups lidded with stone slices were presented in Fig. 9b–d.

All slices of Marble, Qingshi and Hedishi maintained water permeability after treated with protectants, although it is slightly decreased. Water vapor permeability is defined as the mass of water vapor transmitted through a sample per area unit in a time unit (24 h) under defined conditions, and describes the ability of a material to allow water vapor passing through. The following equation was used to calculate the water vapor permeability [12]:

$$WVP = \frac{\Delta M}{(t \times A)}$$

where ΔM is the weight change in the steady state (expressed in g), A is the exposed area to water vapor (in m^2) and t is the unit time (24 h). In all the cases, the used ΔM was the average of three consequent values of the daily difference in weight.

The calculated permeability to water vapor was found to decrease after treated by protectants. For marble slices, reduction of 14.6% and 32.8%was found after treated with colloidal 101S containing1.5 mg/mL Al_2O_3 and 0.1 mg/mL SiO_2 nano-powder. The reductions are slightly higher compared with that of the water colloidal suspension of nanosilica treated Marble which is 26%. Reductions of 53.1% and 50.5% was found for Qingshi stone after treated with 1.5 mg/mL Al_2O_3 and 1.0 mg/mL SiO_2 dispersion in 101S. While that of Hedishi are 55.5% and 40.2% after treated with0.5 mg/mL Al_2O_3 and 1.0 mg/mL SiO_2 dispersion in 101S. It is evident how different results may be obtained from the interactions between nanoparticle dispersions and porous substrates, as a function of a complex of factors, which include the characteristics of both stones and protectants, the application methods and the environmental conditions of the treatments, as well.

Apparent color variation

Usually, color changes induced by protectant treatments are evaluated by a colorimetric analysis using a reflectance colorimeter with a CIE standard illuminant [12]. The measured parameters are L*, a* and b*, where L* accounts for luminosity, a* and b* are coordinates of red-green and blue-yellow. Total color difference (ΔE*) can be calculated by $\Delta E^* = ((\Delta L^*)^2 + (\Delta a^*)^2 + (\Delta b^*)^2)^{1/2}$.

Inherent rich colors and texture patterns exist in the natural stone surfaces. Different parts of the surfaces appear different colors. Hence, it is difficult to evaluate color change by a colorimetric analysis. In present work, the as-prepared colloidal protectants are clear and transparent. The color variation of treated stone surfaces with the protectants is reliably small. Figure 10 shows the optical photos of the blank and treated stone surfaces taken on a same background. Except the inherent difference of the texture patterns of the natural stones, the color of the surfaces shown in Fig. 10 is almost unchanged. Although a colorimetric analysis is not done, we believe the color changes are within the acceptable range, i.e., the total difference is lower than five [13] or lower than three according to other authors [46, 47] who coated similar colloidal dispersions on stone surfaces. The gloss of the

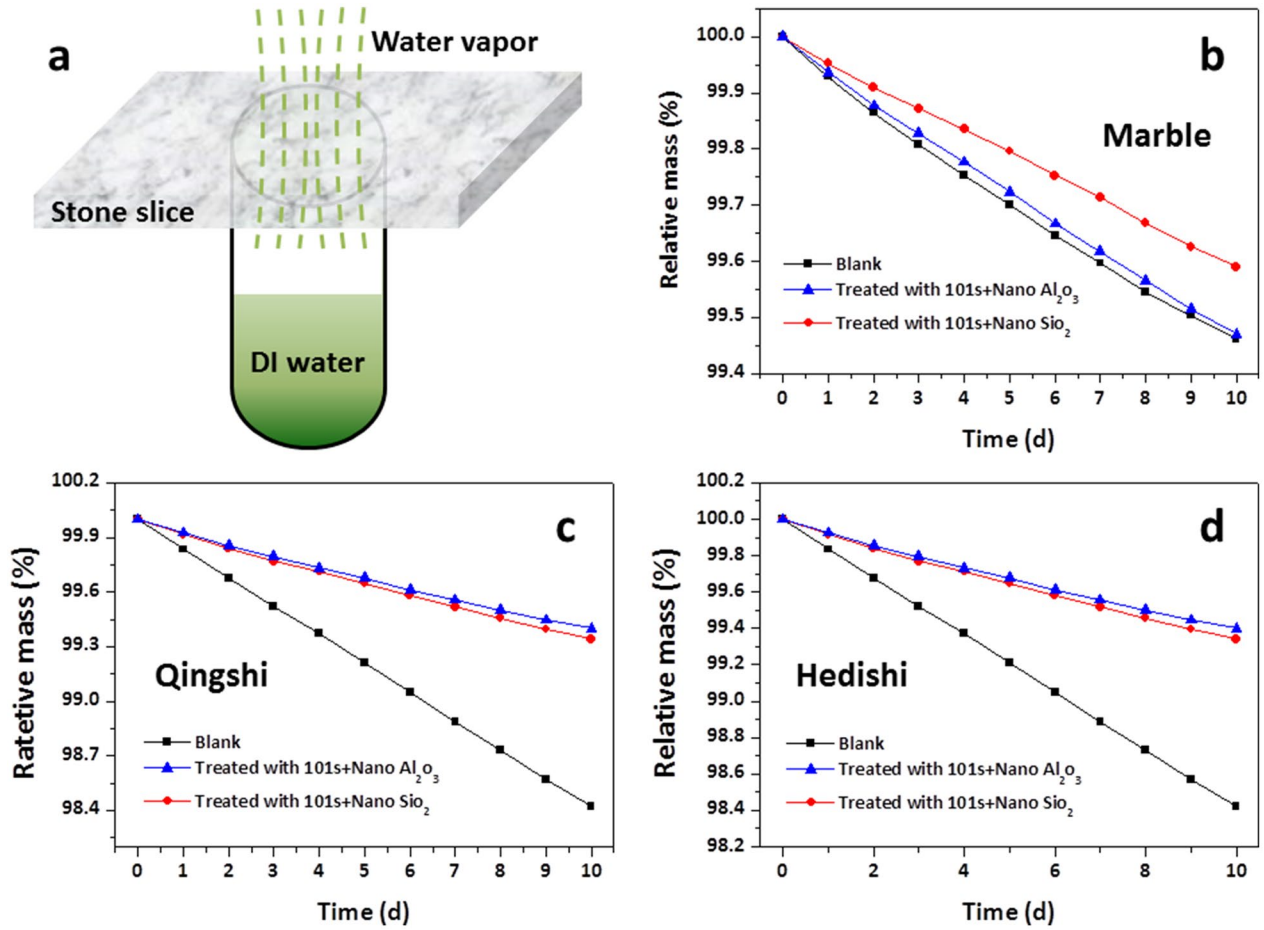

Fig. 9 Schematic diagram of the water vapor permeability experiment (**a**), and relative mass of the cups lidded by stone slices (**b**–**d**). The nano-power concentrations used in the experiments are 1.5 mg/mL Al_2O_3 and 0.1 mg/mL SiO_2 for Marble, 1.5 mg/mL Al_2O_3 and 1.0 mg/mL SiO_2 for Qingshi, and 0.5 mg/mL Al_2O_3 and 1.0 mg/mL SiO_2 for Hedishi, respectively

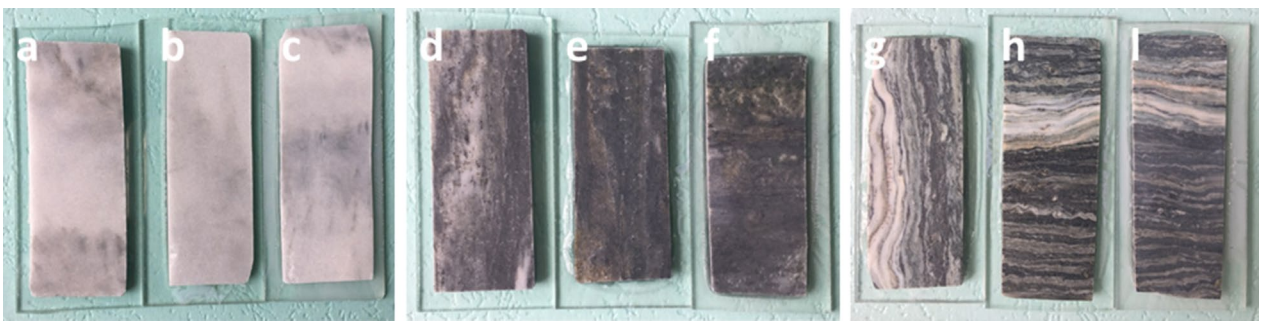

Fig. 10 Optical photos of Marble (**a**–**c**), Qingshi (**d**–**f**) and Hedishi (**g**–**l**) surfaces. For each set of stone surfaces, left to right, they are blank, treated by nano SiO_2 dispersions (1.0 mg/mL for Marbel and Qingshi, 1.5 mg/mL for Hedishi) and nano Al_2O_3 dispersions (1.0 mg/mL for Marbel and Hedishi, 1.5 mg/mL for Qingshi) in 101S, respectively

stone surfaces is lightly dimmed after treatment, mainly come from the nanoscale roughness.

Thermal stability and durability

In order to survey the thermal stability of the as-prepared self-cleaning surfaces, specimens of Marble (treated

by 101S containing 1.5 mg/mL Al_2O_3 and 1.5 mg/mL SiO_2, respectively), Qingshi (treated by 101S containing 0.5 mg/mL Al_2O_3 and 1.0 mg/mL SiO_2, respectively) and Hedishi (treated by 101S containing 2.0 mg/mL Al_2O_3 and 2.0 mg/mL SiO_2, respectively) surfaces were annealed at 100, 150, 200, 250 and 300 °C for 15 min on a hot plate in air, respectively. After naturally cooled to room temperature, the surfaces were subjected to water CAMs.

Figure 11 shows water CAs of the control (without annealing) and the annealed surfaces. The ACAs and SCAs of the surfaces maintained almost unchanged below 250 °C and decreased sharply when the temperature is higher than 250 °C. The RCAs experienced a period of increase below 200 °C and then decrease thereafter. The biggest RCAs rose in the period of 150–200 °C. The surfaces became hydrophilic when annealed at 300 °C, a reflection of decomposition of the 101S. The results agree well with the thermal stability of surfaces coated by fluorinated low surface tension chemicals, indicating the good thermal stability of the as-prepared self-cleaning surfaces [38–40].

The treated stone specimens were placed in outdoor conditions for 9 months (from October 2020 to July 2021), and water CAs were measured. The results are summarized in Table 3 and 4. Compared to the initial data, the SCAs are almost unchanged, while the HAs are slightly increased. The results shown in Table 3 and 4 indicate that the durability of the treated stone surfaces is good and the process developed in this work has actual application value.

Table 3 Water CAs of treated stone surfaces measured in different time. The concentrations of nano Al_2O_3 in 101S are 1.0 mg/mL for Marble and Hedishi, 1.5 mg/mL for Qingshi, respectively

Surface	Time	Treated With 101S + nano Al_2O_3			
		SCA (°)	ACA (°)	RCA (°)	HA (°)
Marble	Oct. 2020	168.9 ± 1.5	170.7 ± 0.3	156.6 ± 0.9	14.1
	Jul. 2021	165.6 ± 0.8	170.0 ± 0.3	154.3 ± 2.3	15.7
Qingshi	Oct. 2020	165.0 ± 1.3	169.2 ± 1.4	153.1 ± 0.5	16.1
	Jul. 2021	165.4 ± 0.7	169.2 ± 1.4	148.1 ± 2.5	21.4
Hedishi	Oct. 2020	165.6 ± 0.1	169.7 ± 0.7	153.0 ± 1.1	16.7
	Jul. 2021	165.7 ± 0.5	170.0 ± 0.9	149.2 ± 4.8	21.0

Conclusions

Inherent microscale interstices and holes exist on the polished natural Marble, Qingshi and Hedishi surfaces. When coated by the commercial protectant, 101S, the surfaces were hydrophobic but not self-cleaning. After being treated by colloidal dispersions of Al_2O_3 and

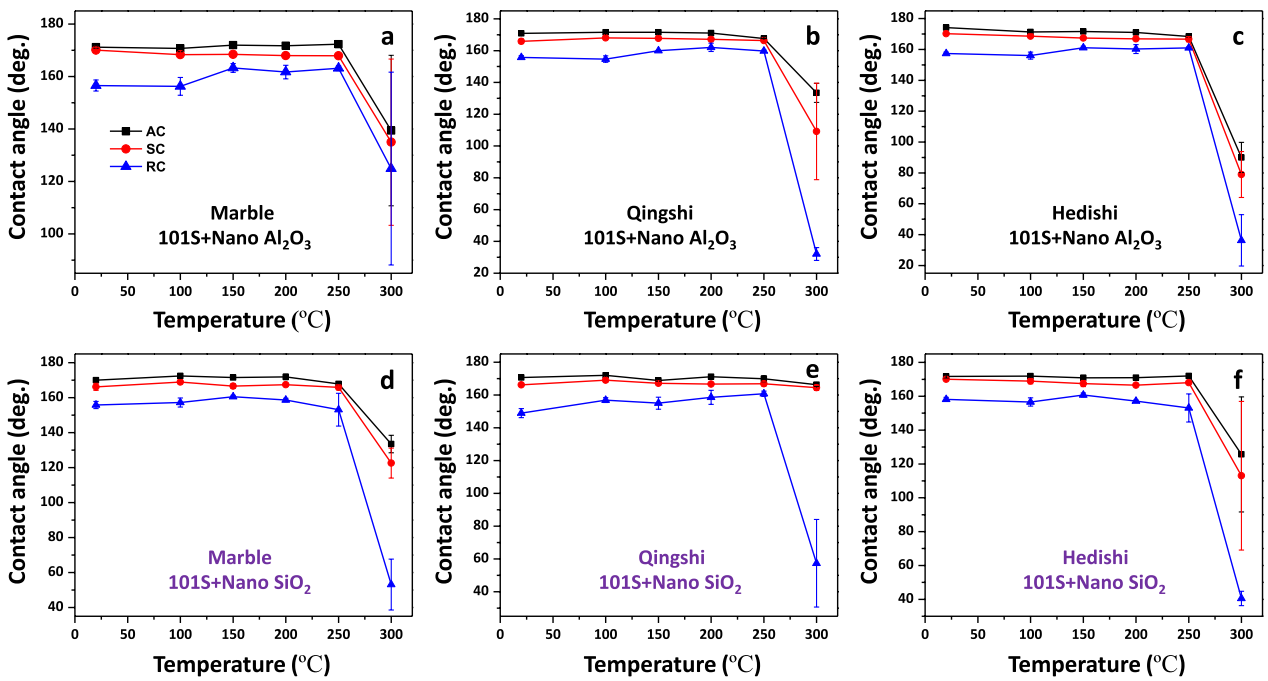

Fig. 11 Variation of water CAs as a function of annealing temperature of the as-prepared self-cleaning surfaces of Marble (**a** and **d**), Qingshi (**b** and **e**) and Hedishi (**c** and **f**) surfaces, respectively

Table 4 Water CAs of treated stone surfaces measured in different time. The concentrations of nano SiO_2 in 101S are 1.0 mg/mL for Marble and Qingshi, 1.5 mg/mL for Hedishi, respectively

Surface	Time	Treated With 101S + nano SiO_2			
		SCA (°)	ACA (°)	RCA (°)	HA (°)
Marble	Oct. 2020	165.4 ± 0.3	167.3 ± 1.4	153.9 ± 1.3	13.4
	Jul. 2021	165.8 ± 0.3	168.3 ± 2.0	150.9 ± 6.3	17.4
Qingshi	Oct. 2020	166.2 ± 0.2	170.6 ± 0.5	150.9 ± 2.8	19.7
	Jul. 2021	165.5 ± 0.3	170.1 ± 0.4	150.0 ± 3.5	20.1
Hedishi	Oct. 2020	169.6 ± 0.1	170.8 ± 0.2	155.3 ± 1.7	15.5
	Jul. 2021	164.0 ± 1.5	166.9 ± 2.0	153.2 ± 3.5	13.8

SiO_2 nano-powder in 101S, self-cleaning surfaces were achieved. Meanwhile, the interstices and holes were reserved.

The nanoparticles provided nanoscale embossments on the inherent microscale structures on the natural stone surfaces to construct micro-nano hierarchical roughness which is the structural base of the self-cleaning surfaces. The principle of the protectants prepared in this work is penetration and crosslinking on the stone surfaces as well as the inner surfaces of the interstices and holes. The reservation of the micro interstices and holes is important since the breathability of the stones can be remained as much as possible. The self-cleaning surfaces showed good thermal stability below 250 °C and damaged with the annealing temperature elevation thereafter.

For the optimal self-cleaning surfaces, the water vapor permeability decreased about 24% for Marble, while that for Qingshi and Hedishi are about 52% and 48%, respectively. The color of the treated surfaces is almost unchanged compared to the blank ones. Little decreases of water CA of the treated stone surfaces were observed after 9 months aging in outdoor conditions, indicating good durability of the self-cleaning surfaces.

Nano-powder addition into water repellence protectants or nanomaterial enhanced protectants provides an easy and effective approach to self-cleaning surfaces of natural stones which will provide an avenue to industrial production for stone surface protection.

Abbreviations

CA: Contact angle; SCA: Static contact angle; ACA: Advancing contact angle; RCA: Receding contact angle; HA: Hysteresis angle; NMEPs: Nano materials enhanced protectants; SEM: Scanning electron microscopy; XRD: X-ray diffraction.

Acknowledgements

The authors thank financial support from National Natural Science Foundation of China (NSFC) and Yunnan Provincial Department of Education Research Fund.

Authors' contributions

ZXX and ZQD: methodology, data curation, original draft preparation. ZQD and BZ: visualization, investigation. DQY and RHL: supervision. YMH: validation, writing—reviewing and editing. All authors read and approved the final manuscript.

Funding

This work was funded by National Natural Science Foundation of China (NSFC) under 11764003 and Yunnan Provincial Department of Education Research Fund under 018JS414 and 2020J0544.

Availability of data and materials

The datasets used and analyzed during the current study are available from the corresponding author on reasonable request.

Declarations

Ethics approval and consent to participate

Not applicable.

Competing interests

The authors declare that they have no competing interests.

Author details

[1]College of Engineering, Dali University, Dali 671003, China. [2]Solmont Technology Wuxi Co., Ltd., 228 Linghu Blvd., Tian'an Tech Park, A1-602, Xinwu District, Wuxi 214135, Jiangsu, China.

Received: 11 May 2021 Accepted: 12 September 2021
Published online: 30 September 2021

References

1. Bonazza A, Messina P, Sabbioni C, et al. Mapping the impact of climate change on surface recession of carbonate buildings in Europe. Sci Total Environ. 2009;407:2039–50.
2. Baedecker PA, Reddy MM. The erosion of carbonate stone by acid rain. J Chem Educ. 1993;70:104–8.
3. Franzoni E, Sassoni E. Correlation between microstructural characteristics and weight loss of natural stones exposed to simulated acid rain. Sci Total Environ. 2012;412/413:278–85.
4. Tecer L. Laboratory experiments on the investigation of the effects of sulphuric acid on the deterioration of carbonate stones and surface corrosion. Water Air Soil Pollut. 1999;114:1–12.
5. Liu Q, Zhang B, Shen Z, Lu H. A crude protective film on historic stone and its artificial preparation through biomimetic synthesis. Appl Surf Sci. 2006;253:2625–32.
6. Corcione CE, Striani R, Frigione M. UV-cured siloxane-modified methacrylic system containing hydroxyapatite as potential protective coating for carbonate stones. Prog Org Coat. 2013;76:1236–42.
7. Cardiano P, Sergi S, Lazzari M, et al. Epoxy-silica polymers as restoration materials. Polymer. 2002;43:6635–40.
8. Corcione CE, Frigione M. Influence of stone particles on the rheological behavior of a novel photopolymerizable siloxane-modified acrylic resin. J Appl Polym Sci. 2011;122:942–7.
9. Ion RM, Turcanu-Caruțiu D, Fierăscu RC, et al. Caoxite-hydroxyapatite composition as consolidating material for the chalk stone for basarabi-murfatlar churches ensemble. Appl Surf Sci. 2015;358:612–8.
10. Matteini M. Inorganic treatments for the consolidation and protection of stone artifacts. Conserv Sci Cult Herit. 2008;8:13–27.
11. Graziania G, Sassonia E, Franzonia E, et al. Hydroxyapatite coatings for marble protection: optimization of calcite covering and acid resistance. Appl Surf Sci. 2016;368:241–57.

12. Vasanelli E, Calia A, Masieri M, et al. Stone consolidation with SiO_2 nanoparticles: effects on a high porosity limestone. Constr Build Mater. 2019;219:154–63.
13. Zornoza-Indart A, Lopez-Arce P. Silica nanoparticles (SiO_2): influence of relative humidity in stone consolidation. J Cult Herit. 2016;18:258–70.
14. Rodriguez-Navarro C, Ruiz-Agudo E. Nanolimes: from synthesis to application. Pure Appl Chem. 2018;90:523–50.
15. Camerini R, Poggi G, Chelazzi D, et al. The carbonation kinetics of calcium hydroxide nanoparticles: a boundary nucleation and growth description. J Colloid Interf Sci. 2019;547:370–81.
16. Carretti E, Chelazzi D, Rocchigiani G, et al. Interactions between nanostructured calcium hydroxide and acrylate copolymers: implications in cultural heritage conservation. Langmuir. 2013;29:9881–90.
17. Facio DS, Mosquera MJ. Simple strategy for producing superhydrophobic nanocomposite voatings in ditu on a building substrate. ACS Appl Mater Interfaces. 2013;5:7517–26.
18. Lazzarini L, Salvadori O. A reassessment of the formation of the patina called "scialbatura." Stud Conserv. 1989;34:20–6.
19. Del Monte M, Sabbioni C, Zappia G. The origin of calcium oxalates on historical buildings monuments and natural outcrops. Sci Total Environ. 1987;67:17–39.
20. Maravelaki-Kalaitzaki P. Black crusts and patinas on pentelic marble from the parthenon and Erechtheum (Acropolis, Athens): characterization and origin. Anal Chim Acta. 2005;532:187–98.
21. Doherty B, Pamplona M, Selvaggi R, et al. Efficiency and resistance of the artificial oxalate protection treatment on marble against chemical weathering. Appl Surf Sci. 2007;253:4477–84.
22. Manoudis PN, Tsakalof A, Karapanagiotis I, et al. Fabrication of superhydrophobic surfaces for enhanced stone protection. Surf Coat Tech. 2009;203:1322–8.
23. Javaheriannaghash H, Ghazavi N. Preparation and characterization of water-based polyurethane–acrylic hybrid nanocomposite emulsion based on a new silane-containing acrylic macromonomer. J Coat Technol Res. 2012;9:323–36.
24. Kapridaki C, Maravelaki-Kalaitzaki P. TiO_2–SiO_2–PDMS nano-composite hydrophobic coating with self-cleaning properties for marble protection. Prog Org Coat. 2013;76:400–10.
25. Melo MJ, Bracci S, Camaiti M, et al. Photodegradation of acrylic resins used in the conservation of stone. Polym Degrad Stab. 1999;66:23–30.
26. Carretti E, Dei L. Physicochemical characterization of acrylic polymeric resins coating porous materials of artistic interest. Prog Org Coat. 2004;49:282–9.
27. Tsakalof A, Manoudis P, Karapanagiotis I, et al. Assessment of synthetic polymeric coatings for the protection and preservation of stone monuments. J Cult Herit. 2007;8:69–72.
28. Favaro M, Mendichi R, Ossola F, et al. Evaluation of polymers for conservation treatments of outdoor exposed stone monuments. Part I: photooxidative weathering. Polym Degrad Stabil. 2006;91:3083–96.
29. Favaro M, Mendichi R, Ossola U, et al. Evaluation of polymers for conservation treatments of outdoor exposed stone monuments. Part II: photo-oxidative and salt-induced weathering of acrylic–silicone mixtures. Polym Degrad Stabil. 2007;92:335–51.
30. Castelvetro V, Aglietto M, Ciardelli F, et al. Structure control, coating properties and durability of fluorinated acrylicbased polymer. J Coat Tech. 2002;74:57–66.
31. Toniolo L, Poli T, Castelvetro V, et al. Tailoring new fluorinated acrylic copolymers as protective coatings for marble. J Cult Herit. 2002;3:309–16.
32. Van Hees RPJ, Brocken HJP. Damage development to treated brick masonry in a long-term salt crystallisation test. Constr Build Mater. 2004;18:331–8.
33. Barthlott W, Neinhuis C. Purity of the sacred lotus or escape from contamination in biological surfaces. Planta. 1997;1:1–8.
34. Neinhuis C, Barthlott W. Characterization and distribution of water-repellent, self-cleaning plant surfaces. Ann Bot. 1997;6:667–77.
35. Tang XD, Yu FQ, Guo WJ, et al. A facile procedure to fabricate nano calcium carbonate–polymer-based superhydrophobic surfaces. New J Chem. 2014;38:2245–9.
36. Zhang H, Zeng XF, Gao YF, et al. A facile method to prepare superhydrophobic coatings by calcium carbonate. Ind Eng Chem Res. 2011;50:3089–94.
37. Zhang H, Liu Q, Liu T, et al. The preservation damage of hydrophobic polymer coating materials in conservation of stone relics. Prog Org Coat. 2013;76:1127–34.
38. Deng R, Hu YM, Wang L, et al. An easy and environmentally-friendly approach to superamphiphobicity of aluminum surfaces. Appl Surf Sci. 2017;402:301–7.
39. Zhao ZE, Sun SH, Hu YM, et al. Robust superamphiphobic aluminum surfaces: fabrication and investigation. J Coat Technol Res. 2019;16:1707–14.
40. Hu YM, Li RH, Zhang XQ, et al. Aluminium films roughened by hot water treatment and derivatized by fluoroalkyl phosphonic acid: wettability studies. Surf Eng. 2020;36:589–600.
41. Wenzel RN. Resistance of solid surface to wetting by water. J Ind Eng Chem. 1936;28:988–94.
42. Wenzel RN. Surface roughness and contact angle. Phys Colloid Chem. 1949;53:1466–7.
43. Cassie A. Contact angles. Discuss Faraday Soc. 1948;3:11–6.
44. Cassie A, Baxter S. Wettability of porous surface. Trans Faraday Soc. 1944;40:546–51.
45. Zhu Y, Hu YM, Nie HY, et al. Superhydrophobicity via organophosphonic acid derivatised aluminium films. Surf Eng. 2016;32:114–8.
46. Benavente D, Martínez-Verdu F, Bernabeu A, et al. Influence of surface roughness on color changes in building stones. Color Res Appl. 2003;28:343–51.
47. Rodrigues JD, Grossi A. Indicators and ratings for the compatibility assessment of conservation actions. J Cult Herit. 2007;8:32–43.

Publisher's Note